AIP | Applied Physics Letters

Spatial distribution of oxygen in luminescent porous silicon films

Omar Teschke

Articles you may be interested in

Study of luminescent porous polycrystalline silicon thin films
J. Vac. Sci. Technol. B **14**, 824 (1996); 10.1116/1.588722

Polarization of porous silicon luminescence
Appl. Phys. Lett. **67**, 3019 (1995); 10.1063/1.114938

Luminescence studies on porous silicon
Appl. Phys. Lett. **63**, 168 (1993); 10.1063/1.110388

Luminescence and structural study of porous silicon films
J. Appl. Phys. **71**, 2403 (1992); 10.1063/1.351097

Luminescence degradation in porous silicon
Appl. Phys. Lett. **60**, 639 (1992); 10.1063/1.106578

Spatial distribution of oxygen in luminescent porous silicon films

Omar Teschke

Instituto de Fisica-UNICAMP 13081-970-Campinas, SP, Brazil

Transmission electron microscopy associated with electron energy loss spectroscopy imaging was used to determine structural spatial variations and compositional variation in heavily doped (0.006 Ω cm) and lightly doped (0.4 Ω cm) luminescent porous silicon films.

Recent studies have shown that an electrochemical etch of silicon produces a microporous material that photoluminesces.[1-3] This visible photoluminescence (PL) has been assigned to quantum confinement effects arising from isolated, nanometer-sized silicon structures produced during the etch process,[1-4] or to the existence of an amorphous phase on the surface of the material.[5,6]

In spite of their degree of interest, the basic formation mechanisms[7] of porous silicon are still in dispute, as well as the puzzling dissolution of silicon occurring preferentially at the tips of the pores and not uniformly over the entire silicon surface. Turner,[8] and subsequently Memming and Schwandt,[9] and Unagami[10] have investigated the formation conditions of porous silicon.

In this letter we used transmission electron microscopy (TEM) associated with electron energy loss spectroscopic imaging (ELSI) for obtaining the compositional distribution and structural variation of porous silicon.

Single-crystal, polished $\langle 100 \rangle$ and $\langle 111 \rangle$ oriented wafers of doped (p-type) silicon of 0.006 (heavily doped) and 0.4 (lightly doped) Ω cm resistivity, respectively, were cut into rectangles with areas of approximately 1.0 cm^2. The etching bath was a solution prepared by admixture of equal volumes of aqueous 48% HF (Merck) and 95% ethanol (Merck). The experimental setup has been previously described.[11] The samples were etched galvanostatically with a model 373A potentiostat/galvanostat (Princeton Applied Research).

After anodization the edge of the silicon slab is gently touched with a 400-mesh TEM specimen grid (parlodium coated) so that fragments of the silicon slab tip are transferred to the specimen grid by capillary adhesion. The grid is dried and inserted into the TEM for study, within a few hours of the anodic fabrication of the tip.

TEM examinations were carried out in a Zeiss CEM902 microscope using 80-keV electrons and equipped with an image intensifying camera. Beam fluxes were as low as possible, to minimize possible specimen damage. ELSI was performed using an appropriate electron energy loss spectrum edge for oxygen and silicon.

Figure 1(a) shows the dimensions and morphology of a typical structure formed by etching ($I=50$ mA/cm^2) $\langle 111 \rangle$ oriented crystalline (p-type, 0.4 Ω cm) silicon. It reveals an array of holes [whitish areas indicated by X in Fig. 1(a)] 25-50 nm across, that form a structure of pores perpendicular to the (111) plane of the silicon slab and exhibit wall dimensions [indicated by Y in Fig. 1(a)] of the order of 10 nm, where columnar dark spots have cross-sectional diameters varying from 12 to 36 Å (indicated by Z).

Figure 1(b) shows the TEM image of a heavily doped silicon $\langle 100 \rangle$ oriented ($\rho = 0.006$ Ω cm, p-type) sample ($I = 200$ mA/cm^2). The structure shows a fine mesh of clear and dark regions where the dark areas are silicon rich and the clear areas are either void or richer in lighter elements. A typical width of the smallest dark structures is 15 Å [marked X in Fig. 1(b)], roughly the smaller diameter observed in Fig. 1(a). Observe that the darker areas in both figures correspond to the sidewalls of the pores. The walls in the $\langle 111 \rangle$ low resistivity sample present a porous structure [see X in Fig. 1(a)] as well as the pore surfaces, while in the $\langle 100 \rangle$ samples mainly the pores [see X in Fig. 1(b)] show a nanometer-sized etched structure.
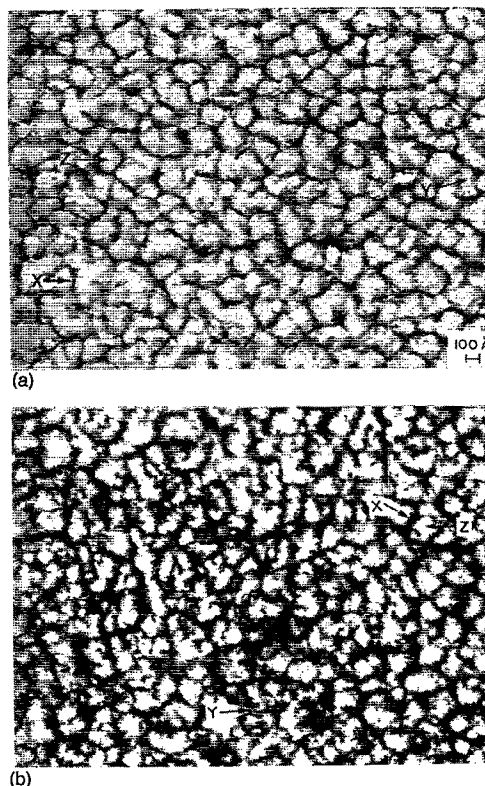

FIG. 1. Transmission electron micrograph of the porous silicon structures formed on (a) p-type lightly doped (0.4 Ω cm) $\langle 111 \rangle$ oriented Si, $I = 50$ mA/cm^2. Y and Z indicate regions with silicon cylinders (dark region) of ~15-Å diameter. X indicates the pore walls dimension. (b) p-type heavily doped (0.006 Ω cm) $\langle 100 \rangle$ oriented Si, $I = 200$ mA/cm^2. Y and Z indicate regions cylinders (dark region) of ~15-Å diameter. X indicates the pore walls dimension.

0003-6951/94/64(15)/1986/3/$6.00
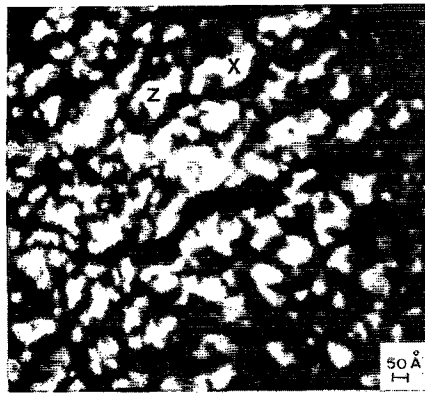
(a)
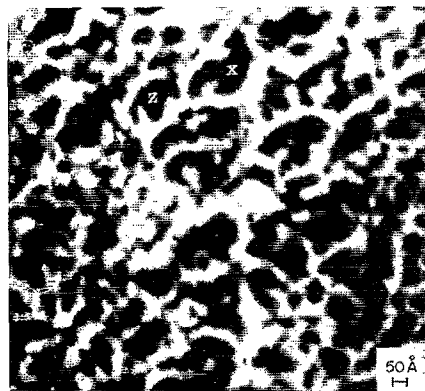
(b)

FIG. 2. (a) Silicon electron energy loss spectroscopic image obtained in type heavily doped ⟨100⟩ oriented Si, $I=200$ mA/cm². X and Z indicate identical points in both images. (b) Oxygen electron energy loss spectroscopic image of the same region as shown in (a).

FIG. 3. Schematic distribution of oxide and hydrogen in porous silicon films. (a) p-type 0.006 Ω cm ⟨100⟩ oriented Si, $I=200$ mA/cm². Sidewalls of the pores are formed by bulk silicon while the bottom shows a nanosized etched structure. (b) p-type 0.4 Ω cm ⟨111⟩ oriented Si, $I=50$ mA/cm². Both side walls and bottom present a nanostructure.

In the ELSI picture the clear areas are regions of high elemental content, and correspondingly, dark regions indicate a hole or a region with low elemental content. Figure 2(a) shows the elemental distribution image of silicon and Fig. 2(b) shows the corresponding oxygen image for a heavily doped Si ⟨100⟩ oriented (p-type, 0.006 Ω cm) sample. X and Z indicate identical points in both images. By comparing the X points in both figures we observe that oxygen-rich structures occupy space devoid of silicon, i.e., the etched bottom of the etched holes. The lightly doped Si ⟨111⟩ oriented (p-type, 0.4 Ω cm) sample did not present any detectable oxygen distribution. Our previous work[12] using IR absorption measurements shows that both heavily doped and lightly doped samples used in this work present large Si-H, Si-H₂, and Si-H₃ absorption band indicating that the top of the anodized layer is hydrogen rich in agreement with previous works.[7,13]

These results may be understood according to the following model. At the start of anodization, inhomogeneities in the region of the semiconductor–electrolyte interface resulting in localization of the current flow, initiate pore formation. Since the top of the surface of the semiconductor is partially covered with Si-H bonds and consequently passivated[14] this layer has a resistance higher than both the electrolyte or the
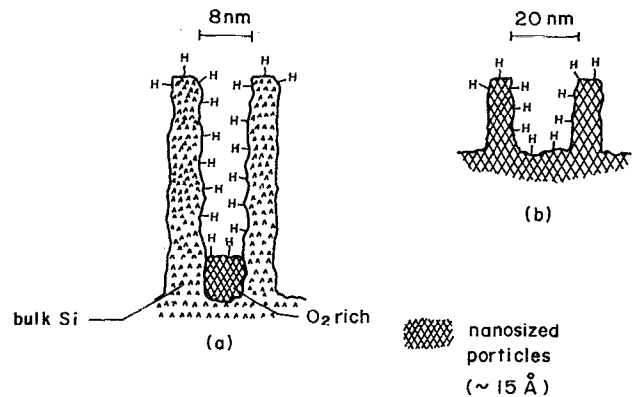
uncovered silicon.[7] Since the formed structure is a porous one, the current has to flow down through the electrolyte into the pores causing oxidation to occur at the pore bottoms, which are, then, oxygen covered. This is experimentally observed for the specimen anodized at high current densities, shown in Fig. 1(b), which has hydrogen at the surface and SiO₂ or siloxenes at the bottom of the holes.

The porous silicon composition for a heavily doped material being different from a lightly doped one may be explained by their different microstructure, i.e., heavily doped samples form pores deeper than lightly doped ones resulting in oxygen being present only at the deepest holes, as shown schematically in Fig. 3.

The walls of the lightly doped samples and the bottoms of the holes are formed by nanosized particles [Fig. 1(a)] covered by hydrogen. These samples exhibit a luminescence peak centered at 1.8 eV when excited by the 2.71-eV line of an Ar ion laser. Electron confinement effects in these structures could be held responsible for the photoluminescence.[6] Heavily doped samples, etched with high current density, also show visible luminescence with a peak centered at 1.9 eV, however our TEM observations of these samples show that the nanosized particles are present but only at the bottom of the etched holes. The origin of the luminescence in this case is not clear for it is impossible to verify whether the luminescence arises from the top surface of the anodized material or from the nanometer-sized particles embedded in oxygen-containing solids, in our experimental setup.

In summary, light-emitting porous silicon films produced by anodization have been further characterized by TEM and ELSI focusing on the oxygen distribution throughout the sample. The porous silicon films formed on lightly doped ⟨111⟩ oriented silicon prepared in this work are composed of an interconnected network of nanometer-size crystalline silicon clusters forming both wall and hole bottoms, while the heavily doped ⟨100⟩ oriented samples show nanosized structures at the bottom of the etched holes only. The surface of the cluster forming the top of the holes is covered with ad-

Omar Teschke 1987

sorbed H atoms in the as-prepared samples. Oxides have been found only at the bottom of the etched holes in heavily doped samples but not in lightly doped ones.

[1] L. T. Canham, Appl. Phys. Lett. **57**, 1046 (1990).

[2] V. Lehmann and U. Gosele, Appl. Phys. Lett. **58**, 856 (1991).

[3] A. G. Cullis and L. T. Canham, Nature **353**, 335 (1991).

[4] A. Bsiesy, J. C. Vial, F. Gaspard, R. Herino, M. Ligeon, F. Muller, R. Romestain, A. Wasiela, A. Halimaoui, and G. Bomchil, Surf. Sci. **254**, 195 (1991).

[5] L. E. Friedersdorf, P. C. Searson, S. M. Prokes, O. J. Glembocki, and J. M. Macauley, Appl. Phys. Lett. **60**, 2285 (1992).

[6] L. R. Tessler, F. Alvarez, and O. Teschke, Appl. Phys. Lett. **62**, 2381 (1993).

[7] R. L. Smith and S. D. Collins, J. Appl. Phys. **71**, R1 (1992).

[8] D. R. Turner, J. Electrochem. Soc. **105**, 402 (1958).

[9] R. Memming and G. Schwandt, Surf. Sci. **4**, 109 (1966).

[10] T. Unagami, J. Electrochem. Soc. **127**, 476 (1980).

[11] O. Teschke, M. C. Goncalves, and F. Galembeck, Appl. Phys. Lett. **63** (1993).

[12] Unpublished.

[13] M. A. Tischler, R. T. Collins, J. H. Stahis, and J. C. Tsang, Appl. Phys. Lett. **60**, 639 (1992).

[14] M. I. J. Beale, J. D. Benjamin, M. J. Uren, N. G. Chew, and A. G. Cullis, J. Cryst. Growth **73**, 622 (1985).